Multi-objective ant lion optimization algorithm to solve large-scale multi-objective optimal reactive power dispatch problem

Article *in* COMPEL International Journal of Computations and Mathematics in Electrical · December 2018

DOI: 10.1108/COMPEL-05-2018-0208

2 authors:


Souhil Mouassa
Universidad de Jaén


Tarek Bouktir
Ferhat Abbas University of Setif

COMPEL - The international journal for computation and mathematics in electrical and electronic engineering

Multi-objective ant lion optimization algorithm to solve large-scale multi-objective optimal reactive power dispatch problem

Souhil Mouassa, Tarek Bouktir,

Multi-objective ant lion optimization algorithm to solve large-scale multi-objective optimal reactive power dispatch problem

Received 9 May 2018
Revised 31 August 2018
Accepted 19 October 2018

Souhil Mouassa and Tarek Bouktir
Department of Electrical Engineering, Faculty of Technology, University of Sétif 1, Sétif, Algeria

Abstract

Purpose – In the vast majority of published papers, the optimal reactive power dispatch (ORPD) problem is dealt as a single-objective optimization; however, optimization with a single objective is insufficient to achieve better operation performance of power systems. Multi-objective ORPD (MOORPD) aims to minimize simultaneously either the active power losses and voltage stability index, or the active power losses and the voltage deviation. The purpose of this paper is to propose multi-objective ant lion optimization (MOALO) algorithm to solve multi-objective ORPD problem considering large-scale power system in an effort to achieve a good performance with stable and secure operation of electric power systems.

Design/methodology/approach – A MOALO algorithm is presented and applied to solve the MOORPD problem. Fuzzy set theory was implemented to identify the best compromise solution from the set of the non-dominated solutions. A comparison with enhanced version of multi-objective particle swarm optimization (MOEPSO) algorithm and original (MOPSO) algorithm confirms the solutions. An in-depth analysis on the findings was conducted and the feasibility of solutions were fully verified and discussed.

Findings – Three test systems – the IEEE 30-bus, IEEE 57-bus and large-scale IEEE 300-bus – were used to examine the efficiency of the proposed algorithm. The findings obtained amply confirmed the superiority of the proposed approach over the multi-objective enhanced PSO and basic version of MOPSO. In addition to that, the algorithm is benefitted from good distributions of the non-dominated solutions and also guarantees the feasibility of solutions.

Originality/value – The proposed algorithm is applied to solve three versions of ORPD problem, active power losses, voltage deviation and voltage stability index, considering large -scale power system IEEE 300 bus.

Keywords Power losses, Particle swarm optimization, Power transmission systems, Voltage stability, Multiobjective optimization

Paper type Research paper

Abbreviation

ALO = Ant lion optimizer;
MOALO = Multi-objective ant lion optimizer;

The authors would like to thank the editors and the six anonymous reviewers for all the constructive and helpful review comments that have helped improved the manuscript significantly. This work was supported by the National CNEPRU project under grant numbers (Grant No: A01L07UN190120140015). The first author expresses his sincere gratitude to Prof. Lucian Toma from the Polytechnic University of Bucharest, Romania for his constructive suggestions.

COMPEL - The international journal for computation and mathematics in electrical and electronic engineering

0332-1649
DOI 10.1108/COMPEL-05-2018-0208

PSO	= Particle swarm optimisation;
MOPSO	= Multi-objective particle swarm optimization;
MOEPSO	= Multi-objective enhanced particle swarm optimization;
NSGA-II	= Non-dominated sorting genetic algorithm II;
ORPD	= Optimal reactive power dispatch;
MOORPD	= Multi-objective optimal reactive power dispatch; and
VEPSO	= Vector Evaluated PSO.

List of Symbols

P_{loss} | VD	= total power losses/voltage deviation;
VSI	= voltage stability index, (*L-index*);
δ_{ij}	= voltage angle difference between i and bus j;
θ_{ji}/V_{Gi}	= phase angle of term F_{ji}/ voltage magnitude for generator at bus i;
N_{PV}, N_{PQ}	= number of PV and PQ buses respectively;
G_k	= conductance of k^{th} branch connected between bus i and j;
V_i, V_j / $V_{L,N_{PQ}}$	= voltage magnitude of bus i and j/Voltage magnitude for load bus i;
$\|Y_{ij}\|/S_i$	= the elements of bus admittance matrix/Apparent power flow of branch i;
$P_{D,i}/Q_{D,i}$	= active/reactive, load consumption at bus i;
P_{Gi}/Q_{Gi}	= active/reactive power generation at bus i;
$P_{L,N_{PQ}}, Q_{L,N_{PQ}}$	= active and reactive power at each load bus;
V_i^{max}, V_i^{min}	= maximum and minimum bus voltage magnitude at bus i;
$Q_{Gi}^{min}, Q_{Gi}^{max}$	= minimum and maximum value of power generation at bus i;
T_k^{max}/T_k^{min}	= maximum/minimum tap ratio of k^{th} tap changing transformer;
$Q_{Ci}^{min}, Q_{Ci}^{max}$	= minimum and maximum VAR injection limits of shunt capacitor banks;
S_i^{max}	= maximum apparent power flow limit of branch i;
NB/NTL	= number of buses in the test system/number of transmission lines;
NLB/NG	= number of load buses/ number of generator buses;
NT/NC	= number of transformer taps/number of shunt capacitor banks;
$\lambda_V, \lambda_Q, \lambda_l$	= penalty factors;
X_i^{lim}	= limit value of the dependent variables V_i^{lim}, Q_i^{lim}, and S_i^{lim};
X_i^{max}/X_i^{min}	= maximum/minimum limit of state variables; and
BCS	= Best compromise solution.

1. Introduction

Optimal reactive power dispatch (ORPD) is a primordial issue in modern electric power systems. It is essential to ensure the stable control and economic operation of power systems. ORPD is a sub-part of the optimal power flow (OPF) problem which consists in determining the optimal adjustment of generator voltage magnitudes, the position of the transformer taps, and the amount of reactive power injected by parallel compensators to minimize active power losses, voltage stability index or voltage deviation while satisfying various physical and operational constraints imposed by the power system itself.

Over the past decade, the electric power system is facing increasing developments due to fundamental changes in both supply and demand, which can affect the security constraints of power system and cause increased losses. These developments force transmission system operators to modify the applied optimization strategies to ensure the economic scheme and to guarantee the satisfaction of all security constraints. These optimization strategies consist of minimizing or maximizing simultaneously two or three conflicting objectives subject to various constraints (Abido and Bakhashwain, 2005) (Khorsandi *et al.*, 2013).

The ORPD is formulated as a multi-objective optimization problem, which aims to minimize simultaneously: the active power losses with index of voltage stability (*L-index*) or the active power losses with the total voltage deviation. In the vast majority of published papers, however, the ORPD problem is dealt with as a single-objective optimization problem (Jordehi, 2017; Mouassa *et al.*, 2017; Naderi *et al.*, 2017; Ng *et al.*, 2017; Rajan *et al.*, 2017) using various conversion methods, such as the weight sum method, epsilon-constraint method and others. These are popularly known as a priori methods. Single-objective optimization approaches are recognized as useful for finding only one best solution to the problem in one program execution or multiple executions to generate a set of Pareto-optimal solutions (Deb, 2011). However, these optimization methods generally encounter some difficulties in identifying the complete or exact Pareto-optimal solutions, especially when it comes to solving complex conflicting objectives (Deb and Saxena, 2006). Furthermore, they are often computationally costly. These difficulties make these methods unsuitable for solving multi-objective optimization problems. In contrast, posterior methods can easily identify a set of Pareto optimal solutions in a single execution and are always capable of determining any kind of Pareto front. However, they are also computationally expensive. On the basis of the detailed literature surveys in (Deb and Saxena, 2018; Dehuri *et al.*, 2015), the multi-objective particle swarm optimization (MOPSO) algorithm, the Non-dominated sorting genetic algorithm (NSGA) and their improved versions are the most widely used ones for solving the MOORPD problem.

In recent years, the ORPD problem has attracted considerable attention in the research community in an effort to ensure the stable and secure operation of electric power systems. At the present time, many published algorithms have been proposed for solving the MOORPD problem (Jeyadevi *et al.*, 2011; Liang *et al.*, 2015). For example, in Jeyadevi *et al.* (2011) the authors proposed a modified NSGA-II considering the strategies of controlled elitism and dynamic crowding distance to improve the diversity of non-dominated solutions. The method was applied on the medium-sized test systems IEEE 30-bus and IEEE 118-bus, but voltage deviation and large-scale test systems were not taken into consideration when validating the technique. An enhanced version of multi-objective PSO to optimize power losses and voltage deviation in power systems was proposed in Chen *et al.* (2016). However, the reported control variables were outside admissible boundaries because the constraint handling method was not properly introduced. Saraswat and Saini (2013) proposed a new hybrid fuzzy multi-objective evolutionary algorithm (HFMOEA) to solve the complex nonlinear multi-objective ORPD problem. Again, however, the robustness of the algorithm was not tested by applying it to a large-scale test system. In Zeng and Sun (2014), an improved version of the MOPSO method was proposed for MOORPD, but the solutions control variables were not discussed. Chen *et al.* (2014) proposed a chaotic improved PSO-based multi-objective optimization to minimize power losses and the voltage stability index, but it was applied only on medium-sized systems, and in addition, almost all the results of the control variables fell outside the imposed limits. Ghasemi *et al.* (2014) derived a new multi-objective algorithm called chaotic parallel vector evaluated interactive honey bee mating optimization (CPVEIHBMO) algorithm to solve the MOORPD problem, but the feasibility of dependent variables was not satisfied. In Liang *et al.* (2015), an improved version of the firefly algorithm to solve the multi-objective active/reactive ORPD problem was presented with load and wind generation uncertainties in a standard IEEE 30-bus system. This test system is insufficient however to confirm the consistency of the proposed algorithm. Again, the optimal control variables were not discussed. Accordingly, the major impediment of these algorithms resides in the inability of dominance to converge to the Pareto frontier while maintaining sufficient diversity. Moreover, due to the complexity of the objective functions used (ORPD problem), they continue to converge toward the local optimum. On the other hand, it obvious to note that is not only interesting to find optimal solution or near optimal solution of such problem, but the most important is to assure the safety constraints and to guarantee that the control variables are within the admissible limits.

The contributions of this paper are twofold. (1) A novel multi-objective algorithm based on the ALO technique for solving the MOORPD problem in large-scale power system is proposed. (2) More importantly, several from existing works on the MOORPD in which the feasibility of solutions were ignored and also not discussed, we therefore, considered three versions of multi-objective ORPD problem where the feasibility of the obtained and reported outcomes are deeply analyzed, discussed and fully verified with the use of power flow calculations.

The ALO algorithm proposed by Mirjalili in 2015 is based on the interactions between ants and ant lions in nature. The multi-objective ant lion optimization (MOALO) algorithm is an extended version of ALO algorithm, and it has been widely used for solving various engineering problems in short time (Li *et al.*, 2018; Cao *et al.*, 2017; Du *et al.*, 2017). The main characteristics of MOALO in terms of convergence, coverage and ability to approximate the global optimum are as follows:

- MOALO algorithm benefits from the high convergence that inherited from the ALO algorithm due to the adaptive boundary shrinking mechanism and operator elitism.
- The use of random walk and roulette wheel give a high capability to avoid getting stuck into a local optimum.
- It presents an appropriate trade-off between exploration and exploitation phases.
- The external archive with the filtering process is first used to store non-dominated Pareto optimal solutions obtained and solutions with lower quality measures are gradually removed from the archive.
- The diversity of solutions is preserved using the niching mechanism to ensure a true Pareto-optimal solution.
- The MOALO algorithm has only three intrinsic parameters to adjust which are the size of the population, the maximum number of iterations and the maximum size of archive.

The results on different benchmarking tests and some engineering problems indicated that not only benefit from high coverage and high convergence, but also superior to other popular multi-objective evolutionary algorithms such as the MOPSO and NSGA-II (Mirjalili *et al.*, 2016). Moreover, there is no application of MOALO algorithm in terms of MOORPD solution involving large-scale power system. The medium-sized IEEE 30-bus, IEEE 57-bus systems and a large-scale IEEE 300-bus system were used to demonstrate the performance of the proposed algorithm. In addition, serious comparatives are done between the MOALO algorithm and enhanced version of MOPSO/original (multi-objective enhanced particle swarm optimization [MOEPSO]/MOPSO) algorithms in terms of the solution quality and the computation efficiency.

2. Problem formulation

The general mathematical formulation of multi-objective optimization can be expressed as follows:

$$\text{Min } \mathbf{F} = \textit{Minimize}\left\{F_1(X),\, F_2(X),\, \ldots\ldots,\, F_n(X)\right\} \tag{1}$$

$$\text{Subject to}:\begin{cases} g_j(X)=0, & j=1,2,\ldots\ldots,k \\ h_j(X)\leq 0, & j=1,2,\ldots\ldots,p \end{cases} \tag{2}$$

where **F** is vector of objective functions, $gj\ (X) = 0$, $h_j\ (X) \leq 0$ are equality and inequality constraints, respectively. The constraints denote the feasible region and vector X at feasible region reflects a feasible solution. In multi-objective ORPD solution provides a set of optimal solutions, instead of one optimal solution, in any two vectors of solution X_1 and X_2, at least one dominates to other or no solution dominates the other. X_1 is dominating X_2 if both the following conditions are met:

$$(i)\forall i\in\{1,\ 2\}:F_i(X_1)\leq F_i(X_2)\quad \text{and}\quad (ii)\exists j\in\{1,\ 2\}:F_j(X_1)<F_j(X_2) \tag{3}$$

The solution X_1 is named the non-dominated solution and the set of the non-dominated solutions form the so-called Pareto front optimal, in which represents the trade-off between the conflicting objectives.

The ORPD is formulated as a multi-objective optimization problem, which minimizes simultaneously the power losses (P_{loss}) and the voltage deviation (VD), or the power losses and the voltage stability index (L-index) as the conflicting objectives while satisfying various equality and inequality constraints (Vlachogiannis and Lee, 2006). Solution of MOORPD problem leads to a set of optimal solutions, instead of one near-optimal solution. Because no solution can be selected to be better than any other with respect to all objective functions, these optimal solutions are define as Pareto optimal solutions. Generally, the mathematical model of the MOORPD problem can be describes as follows:

$$\text{Min F} = \mathit{Minimize}\ \{F_1,\ F_2\}\ \mathit{or}\ \mathit{Minimize}\ \{F_1,\ F_3\} \tag{4}$$

$$\text{Subject to}:\begin{cases} g(x,\ u)=0, & \text{Equality constraints} \\ h(x,\ u)\leq 0, & \text{Inequality constraints} \\ u_j^{lower}\leq u\leq u_j^{upper} & \text{Variable limits} \end{cases} \tag{5}$$

where F_1, F_2, and $F_3$are the objective functions defined in *Section (2.1)*, x is the vector of dependent variables and u is the vector of decision (control) variables. They are expressed as follows:

$$x^T=[V_L\ldots\ldots V_{NLB},\ Q_{G1}\ldots\ldots Q_{G,NG},\ S_1\ldots\ldots S_{NTL}] \tag{6}$$

$$u^T=[V_{G1}\ldots\ldots V_{GNG},\ T_1\ldots\ldots T_{NT},\ Q_{C1}\ \ldots\ldots,\ Q_{CNC}] \tag{7}$$

2.1 Objective functions

2.1.1 Minimization of total active power losses. The total active power loss is minimized (Abou El-Ela *et al.*, 2011). Mathematically it is described as follows:

$$\text{F}_1(x,u)=\min\ P_{\text{Loss}}=\mathit{Minimize}\sum_{k=1}^{NTL}G_k\times\left(V_i^2+V_j^2-2\times V_i\times V_j\times\cos\delta_{ij}\right) \tag{8}$$

2.1.2 Minimization of voltage deviation. This objective function is selected to ensure the security of the electric power system. This is achieved by minimizing the load bus voltage deviations between the reference value and those derived from calculations. Mathematically, it can be defined as:

$$F_2(x,u) = \min \ VD = Minimize \sum_{i=1}^{Npq} |V_i - 1.0| \tag{9}$$

2.1.3 Minimization of voltage stability index. As modern power systems are operated close to their stability limits, the study of voltage stability is becoming an increasingly important factor in power system analysis. The *VSI* was therefore also introduced as an objective function in the present study in an effort to increase the security of electric power systems and to predict voltage collapse. The operating range of the indicator L was set between 0 and 1 (Kessel and Glavitsch, 1986). Therefore, the aforementioned objective can be defined as:

$$F_3(x,u) = \min \ VSI = Minimize(\max(L_j)) \tag{10}$$

where L_j of the j^{th} bus is given by the following expression:

$$L_j = \left| 1 - \sum_{i=1}^{N_{PV}} F_{ji} \times \frac{V_i}{V_j} \angle \{\theta_{ji} + (\delta_i - \delta_j)\} \right| \quad j = 1, 2, \ldots, N_{PQ} \tag{11}$$

with

$$F_{ji} = |F_{ji}| \angle \theta_{ji}, \ V_i = |V_i| \angle \delta_i, \ V_j = |V_j| \angle \delta_j \quad F_{ji} = -[Y_1]^{-1} \times [Y_2] \tag{12}$$

Y_1, Y_2, Y_3, and Y_4 are the sub-matrices of the system Y_{bus} obtained after rearranging the PQ and PV bus bar parameters as shown in equation (13).

$$\begin{bmatrix} I_{PQ} \\ I_{PV} \end{bmatrix} = \begin{bmatrix} Y_1 & Y_2 \\ Y_3 & Y_4 \end{bmatrix} \times \begin{bmatrix} V_{PQ} \\ V_{PV} \end{bmatrix} \tag{13}$$

2.2 System constraints

The objective functions [equations (8)-(10)] are minimized while satisfying the equality and inequality constraints.

2.2.1 Equality constraints include the power flow equations given below.

$$\begin{cases} P_{Gi} - P_{Di} - \sum_{j=1}^{NB} |V_i| \, |V_j| \, |Y_{ij}| \cos(\theta_{ij} - \delta_i + \delta_j) = 0 \\ Q_{Gi} - Q_{Di} - \sum_{j=1}^{NB} |V_i| \, |V_j| \, |Y_{ij}| \sin(\theta_{ij} - \delta_i + \delta_j) = 0 \end{cases} \tag{14}$$

2.2.2 Inequality constraints. These constraints reflect the system operational and the security limits in the power system. They are described below:

- The Reactive power output and the voltage magnitude in each generator and the reactive power supplied by the compensation devices are restricted by their lower and upper limits as follows:

$$\begin{cases} V_{Gi}^{\min} \leq V_{Gi} \leq V_{Gi}^{\max}, & \\ Q_{Gi}^{\min} \leq Q_{Gi} \leq Q_{Gi}^{\max}, & i = 1, 2 \ldots\ldots NG \\ Q_{Ci}^{\min} \leq Q_{Ci} \leq Q_{Ci}^{\max} & i \in NC \end{cases} \tag{15}$$

- For a secure operation of the power system, the voltage magnitudes at load buses and the tap changers of transformers and the apparent power flow of all transmission line are also restricted by their minimum and maximum values as follows:

$$\begin{cases} T_k^{\min} \leq T_k \leq T_k^{\max} & k \in NT \\ V_i^{\min} \leq V_i \leq V_i^{\max} & i \in NB \\ S_i \leq S_i^{\max} & i \in NTL \end{cases} \tag{16}$$

In this work, the control variables are self-constrained, while dependent variables are constrained using the penalty functions, of which only the violating variables (V_i, Q_j, S_i) were added to the objective function to discard any unfeasible solution obtained. Then, the modified objective function of the problem is written as follows:

$$F_{\text{mod}} = F_{obj}(x, u) + \lambda_V \times \sum_{i=1}^{N_{PQ}} \Delta V_i + \lambda_Q \times \sum_{i=1}^{NG} \Delta Q_i + \lambda_l \times \sum_{i=1}^{NTL} \Delta S_i \tag{17}$$

where λ_V, λ_Q and λ_l are the penalty factors; $X_i^{\lim}$is the limit value of the dependent variables that take: $V_i^{\lim}$, $Q_i^{\lim}$, and $S_i^{\lim}$

$$\Delta X_i = \begin{cases} \left(X_i^{\min} - X_i\right)^2 & \text{if } X_i < X_i^{\min} \\ \left(X_i - X_i^{\max}\right)^2 & \text{if } X_i > X_i^{\max} \\ 0 & \text{if } X_i^{\min} \leq X_i < X_i^{\max} \end{cases} \tag{18}$$

3. Multi-objective ant lion optimization algorithm and mathematical formulation

As one of the latest optimization algorithm added to the meta-heuristic list, MOALO was first introduced by Mirjalili *et al.* (2016), which imitates the interactions between ants and antlions in nature. Antlions are a species of predatory insect belonging to the family Myrmeleontidae whose favorite prey is ants. Antlions dig pits in the sand and hide beneath the sand to await their favorite prey; they then devour the ants trapped in the pit with their massive jaws. Moreover, based on the study by Mirjalili *et al.* (2016) the following steps describes the mathematical model of this algorithm.

3.1 Random movement of ants

Ants in nature move stochastically when seeking food. This behavior is expressed mathematically as follows:

$$X(t) = \left[0,\ cumsu(2.r(t_1) - 1),\ cumsu(2.r(t_2) - 1), \ldots\ldots, cumsu\left(2.r(t_{\max\_iter}) - 1\right)\right] \tag{19}$$

where $X(t)$ is the random walk of ants, t is the step of random walk, *cumsu* calculates the cumulative sum and $r(t)$ is a stochastic function defined as follows:

$$r(t) = \begin{cases} 1 & if\ rand > 0.5 \\ 0 & otherwise \end{cases}, rand \in [0,1] \tag{20}$$

As the ants move randomly in the search space [equation (19)], equation (20) is used here in an effort to keep their random movements within the limits of the search space:

$$X_i^t = \frac{(X_i^t - A_i) \times (D_i^t - C_i^t)}{(B_i - A_i)} + C_i^t \tag{21}$$

where A_i, B_i are respectively the minimum and maximum of random walk corresponding to the i^{th} variable. C_i^t, D_i^t are respectively the minimum and maximum of the i^{th} variables at the t^{th} iteration.

3.2 Trapping in the ant lions' traps

The mathematical expression that describes the model of the trapping mechanism is:

$$C_i^t = Antlion_j^t + C^t \tag{22}$$

$$D_i^t = Antlion_j^t + D^t \tag{23}$$

where C^t and D^t indicate respectively the minimum and maximum of all variables in the t^{th} iteration. C_i^t and D_i^t define respectively the minimum and maximum of all variables for the i^{th} ant. $Antlion_j^t$ denotes the position of the selected j^{th} at the t^{th} iteration.

3.3 Building traps

The ALO uses the roulette wheel selection operator to choose antlions based on their fitness. This strategy increases the chances that antlions will trap their prey.

3.4 Sliding ants toward ant lions

For modeling this sliding process, the limits of the random movement should be decreased adaptively by using the following formulas:

$$c^t = \frac{c^t}{I} \tag{24}$$

$$d^t = \frac{d^t}{I} \tag{25}$$

where c^t and d^t, respectively, indicate the minimum and the maximum of all variables at the t^{th} iteration.

I is a ratio, with $I = 10^{w\frac{t}{max\_iter}}$, t is the current iteration and w is the constant which is defined as follows:$w = 2$ when max_*iter* > 0.1, $w = 3$ when max_*iter* > 0.5, $w = 4$ when max_*iter* > 0.75, $w = 4$ if max_*iter* > 0.9, $w = 5$ when max_*iter* > 0.95).

3.5 Catching prey and rebuilding the traps

An ant is trapped in the pit and is then consumed by the antlion, and then the antlion rebuilds new pits to catch the next hunt. This behavior can be modeled as follows:

$$antlion_j^t = ant_i^t, \quad \text{if} \quad fitn\left(ant_i^t\right) \prec fitn\left(antlion_j^t\right) \tag{26}$$

where *fitn* is the fitness value, $antlion_j^t$ denotes the position of the selected j^{th} antlion at the t^{th} iteration and ant_i^t denotes the position of the i^{th} ant at the t^{th} iteration.

3.6 Elitism

Elitism is one of the most important characteristics of evolutionary algorithms. In this algorithm, the best antlion obtained is stored as an elite by which should have an influence on the movements of all the remaining ants during the optimization process. In other words, the random movements on antilions drift around an antlion already chosen by the roulette wheel and the elite antlion The equation to consider both of them is as follows:

$$ant_i^t = \frac{R_A^t + R_E^t}{2} \tag{27}$$

where R_A^t is the random walk around the antlion selected at the t^{th} iteration, R_E^t is the random walk around the elite at the t^{th} iteration, and Ant_i^t denotes the position of the i^{th} ant in the t^{th} iteration. The stopping criterion of this algorithm is the maximum number of iterations.

3.7 Implementation multi-objective ant lion optimization for multi-objective optimal reactive power dispatch problem

The MOALO algorithm is used to solve MOORPD problem, which aims to find the set of optimal solutions of controlled variables by which the solutions found correspond to a minimum value of the selected objective function. The following steps describe the computational procedure for solving the MOORPD problem using the MOALO algorithm and the Figure 1 shows the flowchart of proposed algorithm. In the proposed algorithm, the solution vectors are *antlions* and *ant* and their positions represent the output of each control variables at the MOORPD problem.

Step 1: Define input power system data (line data + bus data) and identify the control variable limits, number of variables, number of search agent, maximum number of iterations, number of Pareto archive.

Step 2: Initialize random values of *ants* and *antlions* populations i.e. for each search agent in population is a randomly generating a string of real values within their control variable limits. Set the generation count (gen = 1).

Step 3: Run power flow algorithm based on the Newton Raphson method for each search agent (*ant* and *antlion*) in an effort to evaluate fitness values corresponding to both objective function (P_{loss} and *VSI* or P_{loss} and *VD*) and constraint violations.

Step 4: Find the best *antlion* and store it as an elite.

Step 5: For each *ant*, select an *antlion* by using Roulette wheel mechanism

Step 6: Search space coverage, i.e. limit of ORPD control variables toward selected *antlion*

Step 7: Create random walk for *ants* (the position of ants here, indicates the control variables of MOORPD problem) to promote the control variables.

Step 8: Update the control variables (position of *ant*) according to Equation (26).

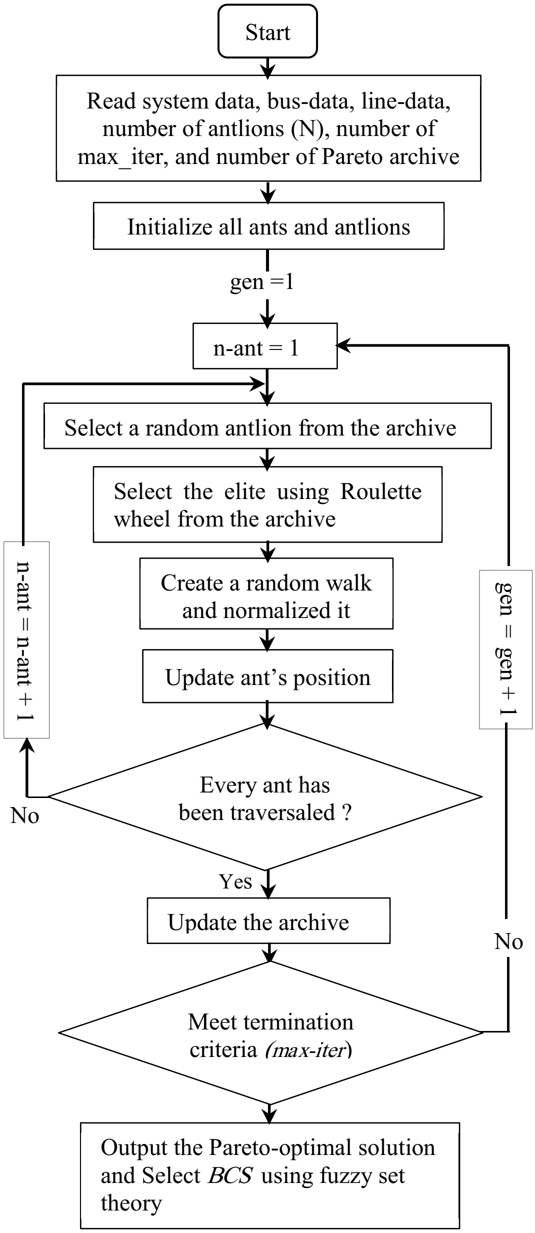

Figure 1.
Flowchart MOALO for MOORPD problem

Step 9: Check if a limit of promoted control variables is within the admissible limit (search space); if so, go to step 11; otherwise go to step 5.

Step 10: Run power flow algorithm based on the Newton Raphson method by utilizing the set of promoted variables to calculate of both objective function values (P_{loss} and VSI or P_{loss} and VD).

Step 11: Replace *antlion* with better *ant* than current *antlion*.

Step 12: Update elite and archive maintenance to realize best Pareto optimal front.

Step 13: Check the stop criterion, i.e. if gen= max generation count, then stop; otherwise increment generation count (gen=gen + 1) and go to step 3.

Step 14: Generate the Pareto optimal front and extract the best compromise solution from the Pareto optimal front using fuzzy set theory.

3.7.1 Best compromise solution (best tradeoff solution). Once having the set of Pareto optimal solutions has been obtained, fuzzy set theory is implemented to extract so-called the best compromise solution that will satisfy the different goals to some extent. In this approach, the membership function μ_i^j for i^{th} objective function F_i of non-dominated solution j is calculated by using the equation below: (Sakawa and Yano, 1987) (Singh and Srivastava, 2015):

$$\mu_i^j = \begin{cases} 1 & F_i \le F_i^{\min} \\ \dfrac{F_i^{\max} - F_i}{F_i^{\max} - F_i^{\min}} & F_i^{\min} < F_i < F_i^{\max} \\ 0 & F_i \ge F_i^{\max} \end{cases} \tag{27}$$

where $F_i^{\max}$and $F_i^{\min}$ are respectively the maximum and the minimum values of the i^{th} objective function among all the non-dominated solutions. The membership function reflects the degree of achievement of the original objective function as a value within [0, 1], i.e. with $\mu^j = 1$ wholly satisfactory and with $\mu^j = 0$ as not satisfactory. For each non-dominated solution j, the membership function is normalized as follows:

$$\mu^j = \frac{\sum_{i=1}^{N_{obj}} \mu_i^j}{\sum_{j=1}^{M} \sum_{i=1}^{N_{obj}} \mu_i^j} \tag{28}$$

where N_{obj} is the number of objective function, and M is the number of non-dominate solutions. The solution with the maximum membership can be considered as the best compromise solution.

4. Simulation results and discussion

In this study, three test systems were used to verify the efficiency and the performance of the proposed algorithm. Five cases, each with different objectives regarding the MOORAD problem, were treated and are summarized as follows:

Case 1: minimization of PLoss and VD in IEEE 30-bus (Chen *et al.*, 2016).

Case 1.1: minimization of PLoss and VD in IEEE 30-bus (Vlachogiannis and Lee, 2005)

Case 2: minimization of PLoss and VD in IEEE 57-bus (Chen *et al.*, 2016).

Case 3: minimization of PLoss and VSI in the IEEE 57-bus (Chen *et al.*, 2014).

Case 4: minimization of PLoss and VD in the IEEE 300-bus;

Case 5: minimization of PLoss and VSI in the IEEE 300-bus.

The algorithm were developed in MATLAB 7.10 programming language and the simulation conducted on a computer Core (TM) i5 a 1.90 GHz with 4 Go RAM. The number of control variables and real power losses in the initial conditions are listed in Table I. The limits on control variables and dependent variables for the first two test systems were taken from (Chen *et al.*, 2014) (Chen *et al.*, 2016), and from (Mouassa *et al.*, 2017) for the large-scale test system.

4.1 EEE 30-bus test system (Chen et al., 2014) (Chen et al., 2016)

This system has six generators at buses 1, 2, 5, 8, 11, 13 (the remaining ones are the PQ buses), four transformers with off-nominal tap ratio at lines 6 − 9, 6 − 10, 4 − 10, and 27 − 28, and, nine parallel compensators at buses 10, 12, 15, 17, 20, 21, 23, 24, and 29 as given in (Lee *et al.*, 1985). The load demand is (2.834+j 1.262) p.u. at 100 MVA base.

4.2 IEEE 57-bus test system (Chen et al., 2014) (Chen et al., 2016)

The standard IEEE 57-bus test system consists of seven generators at buses 1, 2, 3, 6, 8, 9, and 12, eighty of which seventeen transformers with off-nominal tap ratio, and three parallel compensators in buses 18, 25 and 53. The load demand is (12.508+j 3.364) p.u. The complete data can be found in (Zimmerman *et al.*, 2011).

The proposed MOALO algorithm was implemented to solve the MOORPD problem and the outcomes obtained were analyzed and compared with those published using the MOPSO and MOEPSO algorithms. For each of the three electric power systems, 50 independent test runs were performed for solving MOORPD problem using MOALO algorithm.

4.3 Comparison of multi-objective ant lion optimization algorithm with Multi-objective particle swarm optimization and multi-objective enhanced particle swarm optimization algorithms

In first three cases (Cases 1, 1.1, and 2), two competing objective functions, i.e. active power losses and voltage deviation, are optimized simultaneously using MOALO algorithm. The best solution of control variables with results of minimum power loss, minimum voltage deviation, and power loss reduction in per cent and CPU time are listed in Tables II-IV. In addition, under the same variable limits and constraints, the results obtained using MOALO are compared with those reported with the MOPSO and MOEPSO algorithms. From this comparison, it can be seen that MOALO is much more efficient than MOPSO and MOEPSO in terms of solution quality and computation time: with MOALO, the active power losses and voltage deviation for case 2 decreased by about 0.7198 MW and 0.0352 (p.u) compared to those reported with the MOEPSO algorithm. The distribution of the Pareto optimal front for the IEEE 30-bus test system is shown in Figure 2.

Regarding of Case 1.1, the MOALO algorithm is also executed by using all data of ref. (Vlachogiannis and Lee, 2005), the optimal control variables are recorded and compared with those of VEPSO, MOEA in Table II. As shown, the minimal loss of active power is obtained by the proposed MOALO which acquired 4.9818 MW with a reduction of 7.37 per

Table I.
Description of test systems

Parameters	IEEE 30-bus	IEEE57–bus	IEEE 300-bus
number of control variables	19	27	190
number of Generators	6	7	69
number of Taps	4	17	107
number of Qshunt	9	3	14
PLoss(MW)	5.68	28.46	408.316

Variables	MOPSO (Chen *et al.*, 2016) Min PLoss	Min VD	BCS	MOALO Min PLoss	Min VD	BCS
V_{G1}	0.9000	0.9003	1.0957	1.0984	1.0560	1.0802
V_{G2}	1.100	1.1000	1.1000	1.0914	1.0350	1.0719
V_{G5}	1.100	1.1000	1.1000	1.0683	1.0152	1.0438
V_{G8}	1.100	1.1000	1.1000	1.0766	0.9964	1.0481
V_{G11}	1.100	1.1000	1.1000	1.0703	1.0356	1.0614
V_{G13}	1.100	1.1000	1.1000	1.0398	1.0139	1.0304
$T_{6\text{-}9}$	1.04	1.10	1.08	1.0963	1.0272	1.0759
$T_{6\text{-}10}$	0.90	0.90	0.90	1.0368	0.9487	1.0140
$T_{4\text{-}12}$	0.98	1.10	1.04	1.0928	1.0007	1.0677
$T_{28\text{-}27}$	0.96	0.98	0.98	1.0310	0.9630	1.0085
Q_{C10} (MVAR)	5.00	0.50	0.00	4.6403	4.6017	4.6279
Q_{C12}	5.00	5.00	5.00	3.2946	3.7432	3.4322
Q_{C15}	5.00	5.00	5.00	4.1006	4.2643	4.1182
Q_{C17}	5.00	5.00	5.00	2.9287	3.1922	2.9951
Q_{C20}	5.00	5.00	5.00	4.9652	4.9082	4.9045
Q_{C21}	5.00	5.00	5.00	3.3647	3.6315	3.4059
Q_{C23}	5.00	5.00	5.00	3.4841	3.6185	3.4882
Q_{C24}	5.00	5.00	5.00	3.2282	3.5834	3.2965
Q_{C29}	3.50	2.50	2.50	4.9953	4.9441	4.9157
PLoss (MW)	5.1089	5.2069	5.1450	4.7633	5.4267	4.9201
VD (p.u)	0.6130	0.1885	0.2821	0.6371	0.1599	0.3880
% Psave_loss	10.10	8.37	9.46	16.81	4.50	13.42
CPU (s)		53.2			56.1	

Table II. Comparison of simulation results of MOPSO and MOALO for Case 1

Variables	MOEA (Vlachogiannis and Lee, 2005)	VEPSO (Vlachogiannis and Lee, 2005)	MOALO
V_{G1}	1.050	1.0403	1.0759
V_{G2}	1.044	1.1000	1.0638
V_{G5}	1.023	1.0231	1.0395
V_{G8}	1.022	0.9500	1.0434
V_{G11}	1.042	1.0551	1.0415
V_{G13}	1.043	0.9500	1.0386
$T_{6\text{-}9}$	1.090	1.0329	1.0442
$T_{6\text{-}10}$	0.905	0.9913	1.0377
$T_{4\text{-}12}$	1.020 1.020	0.9974	1.0431
$T_{28\text{-}27}$	0.964	1.0165	0.9892
Q_{C10} (MVAR)	Fixed at 19.0	15.056	21.957
Q_{C24} (MVAR)	Fixed at 4.3	3.7842	9.6227
PLoss (MW)	5.1995	5.0941	4.9818
VD (p.u)	0.2512	0.1374	0.3742

Table III. Comparison of simulation results of MOEPSO and MOALO for Case 2

Objectives	MOEPSO (Chen *et al.*, 2016) Min PLoss	Min VD	BCS	MOALO Min PLoss	Min VD	BCS
PLoss (MW)	27.3128	27.7258	27.4268	26.593	27.9679	27.2131
VD (p.u.)	1.0724	0.8459	0.896352	1.1039	0.8107	0.8909
CPU (s)	531.07			115.02		

Table IV. Comparison of simulation results of MOPSO and MOALO for Case 3

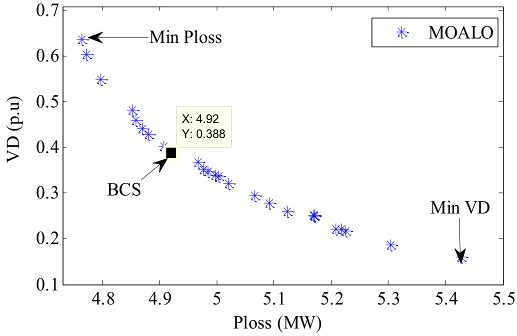

Figure 2.
Pareto optimal front of MOALO, Case 1

cent compared to the initial case, while VEPSO and MOEA reduce power losses by only is 5.29 per cent and 3.33 per cent respectively. For the voltage stability index, our proposed algorithm is a little bit worse than others algorithms. From these results, it can be conclude that the proposed algorithm showed a very competitive performance with respect to the VEPSO and MOEA.

For Case 3, the optimum values of power losses and voltage stability index (*L-index*) obtained with MOALO were 26.3952 MW and 0.2854, i.e. 16 and 1.02 per cent less than those reported with MOPSO, respectively. Furthermore, the computational time for MOALO was less than for the MOPSO and MOEPSO algorithms for Case 2 and Case 3, but a little worse for case 1. The reactive power outputs of generators corresponding to the MOORPD solution obtained by the proposed MOALO for cases 2, and 3 are presented in Figures 4-5. Figure 3 depicts the voltage profile of case 2. These results amply confirm the capability of the proposed algorithm to handle the equality and inequality constraints of the MOORPD problem.

To further assess the results obtained and to highlight the value of the MOALO algorithm in solving the constrained MOORPD problem, the accuracy of the results reported with the MOPSO and MOEPSO algorithms as well those obtained with the MOALO algorithm were checked, specifically those of the dependent variables (reactive power outputs of generators and load bus voltages). The outcomes were recalculated by using the corresponding optimal control variables of each simulation case as input data of the Matpower load flow program.

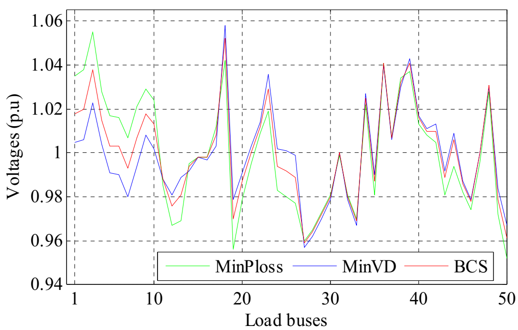

Figure 3.
Voltage profile for IEEE 57-bus system, Case 2, P_{loss} and *VD*

The exact results of P_{Loss}, *VD,* and *L-index* obtained from the power flow program for the three cases are summarized in Table VI. A meticulous observation of these results reveals a violation of the dependent variables' limits, rendering the solutions infeasible. An in-depth critical analysis of the reported results was carried out on the IEEE 30-bus and IEEE 57-bus test systems and can be summarized as follows:

- *Case 1 – min* P_{Loss}: The reactive power of generators at buses 1, 2, and 8 violates their limits by 95.14 per cent, 95.26 per cent, and 31.81 per cent respectively. Also, all the voltage magnitudes at the load buses except buses 3 and 4 exceed the fixed limits [0.94 – 1.06] p.u.
- *Case 2 – min VD*: The reactive power of generators in all PV buses except 12 violates their limits by 79.26 per cent, 95.51 per cent, 94.71, 42.92, and 99.67 per cent respectively. Also, almost all voltage magnitudes at the load buses exceed the upper and lower limits [0.94 – 1.06] p.u. In addition, the exact values of power loss and voltage deviation are 134.634 MW and 3.8182 (p.u) respectively. Therefore, there are significant differences between reported and recalculated results.
- *Case 3 – min VSI*: The reactive power of generators at all buses 1, 2, 3, 6, 8, 9, and 12 violates their limits by 73.26 per cent, 97.77 per cent, 86.78 per cent, 60.93 per cent, 39.20 per cent, 78.46 per cent, and 41.16 per cent respectively. Furthermore, the voltage magnitudes at the load buses 7, 8, 16–18, 43–48, 51 exceed the voltage limits [0.94 – 1.06] p.u.

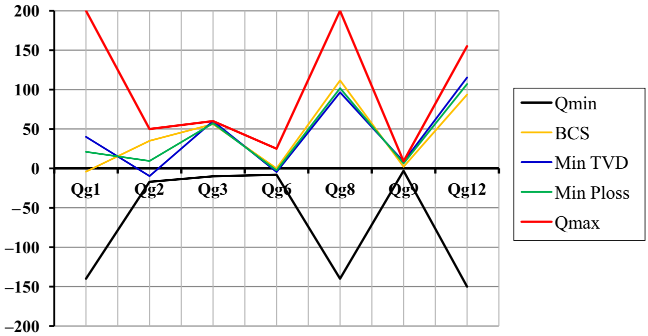

Figure 4.
Reactive power outputs at generators for Case 2, IEEE-57 bus system

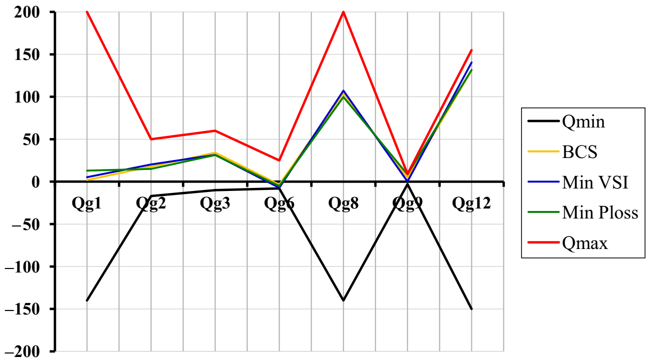

Figure 5.
Reactive power outputs at generators for Case 3, IEEE-57 bus system

Table V. Comparison of simulation results of MOPSO and MOALO for 57-bus system

	MOPSO (Chen *et al.*, 2014)			MOALO		
Variables	Min PLoss	Min VSI	BCS	Min PLoss	Min VSI	BCS
V_{G1}	1.10000	1.10000	1.10000	1.0638	1.0456	1.0550
V_{G2}	0.90000	0.90000	0.90000	1.0486	1.0298	1.0381
V_{G3}	1.10000	1.10000	1.10000	1.0510	1.0297	1.0383
V_{G6}	1.10000	0.99771	1.05681	1.0570	1.0336	1.0424
V_{G8}	0.90000	0.90000	0.90000	1.0967	1.0764	1.0830
VG9	1.08959	0.96893	1.05494	1.0666	1.0462	1.0552
$V_{G1}2$	1.10000	1.10000	1.10000	1.0805	1.0642	1.0701
T4-18	0.90000	0.90000	0.90000	1.0195	0.9978	1.0053
T4-18	0.97000	1.00000	1.01000	1.0340	1.0112	1.0210
T21-20	1.01000	1.10000	1.04000	1.0990	1.0952	1.0983
T24-25	0.90000	0.90000	0.90000	0.9909	0.9642	0.9735
T24-25	1.10000	1.10000	1.10000	1.0128	0.9844	0.9934
T24-26	1.10000	1.10000	1.10000	1.0998	1.0947	1.0977
T7-29	0.91000	0.91000	0.91000	0.9973	0.9693	0.9799
T34-32	0.90000	0.90000	0.90000	1.0305	1.0029	1.0136
T11-41	0.90000	0.9000	0.90000	1.0260	1.0057	1.0138
T15-45	0.92000	0.9200	0.92000	0.9904	0.9642	0.9737
T14-46	0.90000	0.9000	0.90000	0.9828	0.9579	0.9672
T10-51	0.90000	0.9000	0.90000	0.9963	0.9759	0.9853
T13-49	1.10000	1.1000	1.10000	1.0084	0.9902	0.9988
T11-43	0.91000	0.9100	0.91000	0.9987	0.9738	0.9825
T40-56	1.10000	1.1000	1.10000	1.0291	1.0038	1.0140
T39-57	0.97000	1.0300	1.01000	0.9995	0.9765	0.9864
T9-55	0.92000	0.9200	0.92000	1.0650	1.0421	1.0525
QC18 (MVAR)	7.500	18.50	17.50	5.8080	5.8077	5.8632
QC25(MVAR)	0.000	0.000	0.000	8.6317	8.3751	8.4914
QC53(MVAR)	0.000	0.000	0.000	13.5386	13.3489	13.4402
PLoss (MW)	31.424	31.595	31.462	26.3952	27.2634	26.7477
VSI	0.29123	0.28834	0.28952	0.2994	0.2854	0.2885
CPU (s)	424.59			151.55		

Table VI. Results of power flow for control variables given in Tables II-IV

Algorithms		Calculated PLoss	VD	Violating constraints Load buses	QG
min PLoss	Case 1MOPSO	36.993	2.137	all buses except 3 and 4	1,2, and 8
min VD		36.971	1.54	4, 6, 10, 17, 25, 27, 28, 29	1, 2, 3
BCS		4.836	2.027	all buses	1
min PLoss	Case 2MOEPSO	123.78	2.976	12-20, 24,26, 27, 30, 31,34-39, 55, 57	1-3, 6, 8, 9,12
min VD		134.63	3.818	4, 5, 13-28, 30-44, 55	all except 12
BCS		149.62	2.964	4, 5, 11-17, 19-26, 30-40, 55	all except 12
min PLoss	Case 3MOPSO	117.98	VSI 0.249	4, 5, 11, 13-25, 32, 33, 36-51, 54-57	all except 12
min VSI		105.44	0.273	7, 8, 16-18, 43-48, 51	1-3, 6, 8, 9,12
BCS		109.52	0.256	4, 8, 13,15-24, 32, 33, 38, 41,43-48, 50,51,55	all except 12

The same verifications were performed for all the remaining cases, and significant differences between the power flow outcomes obtained and the corresponding results reported in references (Chen *et al.*, 2014) and (Chen *et al.*, 2016) were found (see Table VI). These solutions are therefore judged to be infeasible due to the undesirable violation of dependent variables. On other hand, just a glance at Figure 3 and Table V is sufficient to confirm the consistency of the proposed algorithm of finding the best solutions while satisfying the power flow equations, system security, and equipment operating limits.

4.4 Large-scale test system, IEEE 300-bus

To examine the capability of MOALO algorithm to solve the MOORPD problem in a large-scale power system, the IEEE 300-bus (Zimmerman *et al.*, 2011) was used as the test system. It consists of 69 generators, 411 transmission lines of which 107 branches with off-nominal tap ratios. In addition, 14 parallel compensators were considered as given in (Mazzini, 2016) (Mouassa *et al.*, 2017). The total load demand is (235.258 + j77.8797) p.u. The min/max of the control vector were taken from (Mouassa *et al.*, 2017). Moreover, it is important to note that this test system exhibits very large voltage drops (Coffrin *et al.*, 2014), making it harder to ensure the feasibility of solutions.

4.5 Discussion

Und er the constraints used here, the P_{loss} and VD were optimized simultaneously as multi-objective functions on a large-scale IEEE 300-bus system. The Pareto optimal front obtained using MOALO is depicted in Figure. 6. The optimal values of reactive power sources and the P_{Loss}, VD, and best compromise solution (BCS) are listed in Table VII that also satisfies system security. Power losses and voltage deviation were reduced by 3.63 per cent and 4.76 per cent respectively with respect to the base case. The average computation time required to attain a near-optimal solution for the large-scale power system was 23.8 seconds per iteration. In addition, from Figure 6, it can be seen that the optimal Pareto front has a good distribution of the non-dominated solutions, thus validating the potential of MOALO algorithm to solve the nonlinear multi-objective problem.

For Case 5, the optimum values for power losses and voltage stability index obtained with the MOALO algorithm were 384.51 MW and 0.1983 respectively, i.e. a reduction of 5.83 per cent and 52 per cent respectively compared with the base cases. It is necessary to note that the voltages magnitudes at all of load buses are inside the imposed boundaries. Therefore, according to Table VII, the reactive powers of the parallel compensators are within the admissible limits, confirming the efficiency of the proposed algorithm to obtain the feasible solutions. Figure 7 shows the distribution of non-dominant solutions that correctly represent the Pareto optimal front.

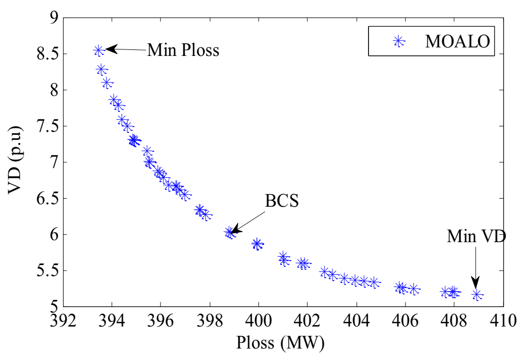

Figure 6.
Pareto optimal front of MOALO, Case 4

	IEEE 300-bus system								
	Limits			Case 4			Case 5		
Variables	Qmin	Qmax	Min PLoss	Min VD	BCS	Min PLoss	Min VSI	BCS
Q_{96}	0	4.5	3.661	3.614	3.638	1.991	1.915	1.962
Q_{99}	0	0.59	0.4218	0.4176	0.4188	0.509	0.500	0.506
Q_{133}	0	0.59	0.3108	0.3087	0.3085	0.444	0.433	0.440
Q_{143}	−4.5	0	−4.3382	−4.2047	−4.251	−2.574	−2.621	−2.59
Q_{145}	−4.5	0	−2.4711	−2.3514	−2.4021	−3.377	−3.428	−3.95
Q_{152}	0	0.59	0.1534	0.1471	0.1503	0.1721	0.1629	0.1685
Q_{158}	0	0.59	0.5589	0.5539	0.5543	0.5325	0.5163	0.5274
Q_{169}	−2.5	0	−1.2811	−1.2306	−1.2443	−2.231	−2.262	−2.238
Q_{210}	−4.5	0	−3.036	−2.935	−2.989	−4.194	−4.214	−4.201
Q_{217}	−4.5	0	−3.991	−3.904	−3.938	−3.305	−3.386	−3.328
Q_{219}	−1.5	0	−0.6356	−0.5987	−0.6115	−0.8038	−0.8135	−0.807
Q_{227}	0	0.59	0.5059	0.4957	0.4983	0.375	0.362	0.369
Q_{268}	0	0.15	0.1143	0.1125	0.1131	0.1180	0.1157	0.1170
Q_{283}	0	0.15	0.0868	0.08560	0.0860	0.0847	0.0825	0.0839
P_{Loss}			393.4646	408.899	398.8527	384.5104	392.7140	386.241
VD			8.5482	5.1702	6.0169			
L-index						0.2058	0.1983	0.2010

Note: P_{Loss}: (MW); VD: (p.u);VSI: L-index; Q_g:(p.u);V(p.u)

Table VII. Reactive power outputs of parallel compensators for IEEE 300-bus, Case 4

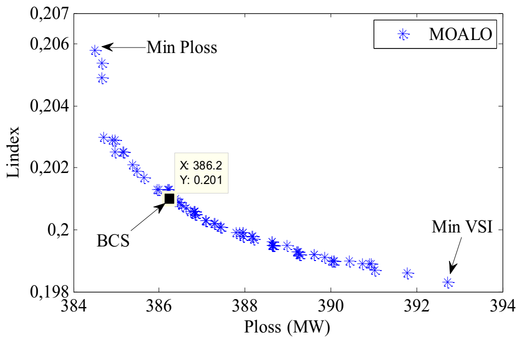

Figure 7. Pareto optimal front of MOALO algorithm, Case 5

As a result, even with the large-scale test system, the MOALO algorithm gives the best adjustment of control variables and converges well to the Pareto front with a good diversity of solutions. In other words, it has been also proven that the proposed MOALO algorithm is more suitable to solve MOORPD than the other algorithms of which it can not only benefit from good distributions of the non-dominated solutions, but also guarantee the feasibility of solutions obtained for three test power systems.

5. Conclusion

The work presented in this paper investigates the applicability of MOALO algorithm in solving the large-scale MOORPD problem in an effort to improve the performance of power systems operation and reduce active power losses by accurate adjustment of control variables. The ORPD problem is a complex multi-objective optimization problem that involves independent decision variables and multiple conflicting objectives. The findings to this study make many contributions of the current literature: The conflicting objectives, namely real power loss, voltage deviation, and voltage stability index were successfully minimized under various constraints. The proposed algorithm was successfully tested on standard IEEE 30-bus and IEEE 57-bus test systems, and on a large-scale IEEE 300-bus system. An in-depth analysis on the both obtained and reported results was presented, verified and approved the feasibility of solutions. The MOALO results were compared with those of the other heuristic methods reported in the literature, namely MOPSO, MOEPSO and VEPSO. The comparison indicates that the MOALO is much more effective than these algorithms in terms of the quality of obtained optimal solutions and simulation time required. Moreover, simulation results obviously demonstrate the capabilities of the proposed algorithm to generate a set of non-dominated feasible solutions (Pareto optimal). The proposed algorithm therefore shows a good ability to solve the complex multi-objective optimization problem, even in the case of large-scale power systems. Thus, the MOALO algorithm may be recommended as a very promising tool for solving some more other complex engineering optimization problems for the future researchers. With regard to future extensions of this work, the authors propose the possibility to minimize the total cost paid by the system operator to the generators for providing the required reactive power support with the presence of the intermittent sources.

References

Abido, M.A. and Bakhashwain, J.M. (2005), "Optimal VAR dispatch using a multiobjective evolutionary algorithm", *International Journal of Electrical Power and Energy Systems*, Vol. 27 No. 1, pp. 13-20.

Abou El-Ela, A.A., Kinawy, A.M., El-Sehiemy, R.A. and Mouwafi, M.T. (2011), "Optimal reactive power dispatch using ant colony optimization algorithm", *Electrical Engineering*, Vol. 93 No. 2, pp. 103-116.

Cao, W.D., Yan, C.P., Wu, D.J. and Tuo, J.B. (2017), "A novel multi-objective optimization approach of machining parameters with small sample problem in gear hobbing", *The International Journal of Advanced Manufacturing Technology*, Vol. 93 Nos 9/12, pp. 4099-4110.

Chen, G., Liu, L. and Yanyan Guo, S.H. (2016), "Multi-objective enhanced PSO algorithm for optimizing power losses and voltage deviation in power systems", *Compel - the International Journal for Computation and Mathematics in Electrical and Electronic Engineering*, Vol. 35 No. 1, pp. 350-372.

Chen, G., Liu, L., Song, P. and Du, Y. (2014), "Chaotic improved PSO-based multi-objective optimization for minimization of power losses and L index in power systems", *Energy Conversion and Management, Elsevier Ltd*, Vol. 86, October, pp. 548-560.

Coffrin, C. Gordon, D. and Scott, P. (2014), "NESTA, the NICTA energy system test case archive", arXiv:1411.0359 [Cs], pp. 1-26.

Deb, K. (2011), "Multi-objective optimization using evolutionary algorithms: an introduction", pp. 1-24.

Deb, K. and Saxena, D.K. (2018), "On finding pareto-optimal solutions through dimensionality reduction for certain large-dimensional multi-objective optimization problems EMO for many objectives", Technical Report, KanGAL Report No. 2005011.

Dehuri, S., Jagadev, A.K., Panda, M. and Advances, T. (2015), *Multi-Objective Swarm Intelligence: Theoretical Advances and Applications*, Dehuri, S., Jagadev, A.K. and Panda, M. (Eds), 1st–2015th ed., Springer-Verlag Berlin Heidelberg, Odisha, India, available at: https://doi.org/10.1007/978-3-662-46309-3

Du, P., Wang, J., Guo, Z. and Yang, W. (2017), "Research and application of a novel hybrid forecasting system based on multi-objective optimization for wind speed forecasting", *Energy Conversion and Management, Elsevier*, Vol. 150, July, pp. 90-107.

Ghasemi, A., Valipour, K. and Tohidi, A. (2014), "Multi objective optimal reactive power dispatch using a new multi objective strategy", *International Journal of Electrical Power and Energy Systems, Elsevier*, Vol. 57, May, pp. 318-334.

Jeyadevi, S., Baskar, S., Babulal, C.K. and Iruthayarajan, M.W. (2011), "Electrical power and energy systems solving multiobjective optimal reactive power dispatch using modified NSGA-II", *International Journal of Electrical Power and Energy Systems*, Elsevier Ltd, Vol. 33 No. 2, pp. 219-228.

Jordehi, R. (2017), "Gaussian bare-bones water cycle algorithm for optimal reactive power dispatch in electrical power systems", *Applied Soft Computing Journal*, Elsevier B.V., Vol. 57, August, pp. 657-671, available at: https://doi.org/10.1016/j.asoc.2017.04.048

Kessel, P. and Glavitsch, H. (1986), "Estimating the voltage stability of a power system", *IEEE Transactions on Power Delivery*, Vol. 1 No. 3, pp. 346-354.

Khorsandi, A., Hosseinian, S.H. and Ghazanfari, A. (2013), "Modified artificial bee colony algorithm based on fuzzy multi-objective technique for optimal power flow problem", *Electric Power Systems Research*, Elsevier B.V, Vol. 95, pp. 206-213.

Lee, K.Y., Park, Y.M. and Ortiz, J.L. (1985), "A united approach to optimal real and reactive power dispatch", *IEEE Power Engineering Review*, Vol. PER-5 No. 5, pp. 42-43.

Li, Y., Feng, B., Li, G., Qi, J., Zhao, D. and Mu, Y. (2018), "Optimal distributed generation planning in active distribution networks considering integration of energy storage", *Applied Energy, Elsevier*, Vol. 210 No. July, pp. 1073-1081.

Liang, R., Wang, J., Chen, Y. and Tseng, W. (2015), "An enhanced firefly algorithm to multi-objective optimal active/reactive power dispatch with uncertainties consideration", *International Journal of Electrisscal Power And Energy Systems*, Elsevier Ltd, Vol. 64, January, pp. 1088-1097.

Mazzini, A.P. (2016), "Development of continuous and discrete optimization strategies to problems of optimal power flow", thesis doctorate, UNIVERSIDADE DE SÃO PAULO.

Mirjalili, S., Jangir, P. and Saremi, S. (2016), "Multi-objective ant lion optimizer: a multi-objective optimization algorithm for solving engineering problems", *Applied Intelligence, Applied Intelligence*, Vol. 46 No. 1, pp. 79-95.

Mouassa, S., Bouktir, T. and Salhi, A. (2017), "Ant lion optimizer for solving optimal reactive power dispatch problem in power systems", *Engineering Science and Technology, an International Journal*, Vol. 20 No 3, available at: https://doi.org/10.1016/j.jestch.2017.03.006

Naderi, E., Narimani, H., Fathi, M. and Narimani, M.R. (2017), "A novel fuzzy adaptive configuration of particle swarm optimization to solve large-scale optimal reactive power dispatch", *Applied Soft Computing Journal*, Elsevier B.V., Vol. 53, April, pp. 441-456, available at: https://doi.org/10.1016/j.asoc.2017.01.012

Ng, R., Mei, S., Herwan, M., Mustaffa, Z. and Daniyal, H. (2017), "Optimal reactive power dispatch solution by loss minimization using moth-flame optimization technique", *Applied Soft Computing Journal*, Elsevier B.V, Vol. 59, pp. 210-222.

Rajan, A., Jeevan, K. and Malakar, T. (2017), "Weighted elitism based ant lion optimizer to solve optimum VAr planning problem", *Applied Soft Computing Journal*, Elsevier B.V., Vol. 55, June, pp. 352-370, available at: https://doi.org/10.1016/j.asoc.2017.02.010

Sakawa, M. and Yano, H., Yumine, T. (1987), "An interactive fuzzy satisficing method for multiobjective linear-programming problems and its application", *IEEE Transactions on Systems, Man, and Cybernetics*, Vol. 17 No. 4, pp. 654-661.

Saraswat, A. and Saini, A. (2013), "Multi-objective optimal reactive power dispatch considering voltage stability in power systems using HFMOEA", *Engineering Applications of Artificial Intelligence*, Vol. 26 No. 1, pp. 390-404.

Singh, H. and Srivastava, L. (2015), "Recurrent multi-objective differential evolution approach for reactive power management", *IET Generation, Transmission and Distribution*, Vol. 10 No. 1, pp. 1-13.

Vlachogiannis, J.G. and Lee, K.Y. (2005), "Reactive power control based on particle swarm Multi-Objective optimization", *Proceedings of the 13th International Conference On, Intelligent Systems Application to Power Systems*, *Arlington, VA*, 6-10 November, pp. 494-498.

Vlachogiannis, J.G. and Lee, K.Y. (2006), "A comparative study on particle swarm optimization for optimal Steady-State performance of power systems", *IEEE Transactions on Power Systems*, Vol. 21 No. 4, pp. 1718-1728.

Zeng, Y. and Sun, Y. (2014), "Solving multiobjective optimal reactive power dispatch using improved multiobjective particle swarm optimization", *Control and Decision Conference (2014 CCDC), The 26th Chinese*, *IEEE*, *Changsha, China*, 31 May-2 June, pp. 1010-1015.

Zimmerman, R.D., Murillo Sa¨nchez, C.E. and Thomas, R.J. (2011), "MATPOWER: Steady-State operations, planning, and analysis tools for power systems research and education, power systems", *IEEE Transactions on Power Systems*, Vol. 26 No. 1, pp. 12-19.

About the authors

Souhil Mouassa is an Assistant Lecturer at Bouira University (Algeria). He received BS and MS in Electrical Engineering Power System from Sétif University (Algeria) in 2009 and 2012, respectively. He is pursuing PhD from the University of Ferhat Abbas Sétif 1, Algeria. His research focuses on power system networks, FACTS, optimal power flow and power system optimization, demand response and smart grids. Souhil Mouassa can be contacted at: mouassa@univ-setif.dz

Tarek Bouktir was born in Ras El-Oued, Algeria, in 1971. He received BS in Electrical Engineering Power System from Setif University (Algeria) in 1994, MSc from Annaba University in 1998 and PhD in Power System from Batna University (Algeria) in 2003. His areas of interest are applications of meta-heuristic methods in optimal power flow, FACTS control and improvement in electric power systems, multi-objective optimization for power systems and voltage stability and security analysis. He is the Editor-In-Chief of *Journal of Electrical Systems* (Algeria), the co-editor of the *Journal of Automation & Systems Engineering* (Algeria). He currently serves on the editorial boards of *Leonardo Electronic Journal of Practices* (Romania) *and Technologies*, *Leonardo Journal of Sciences* (Romania), *WSEAS Transactions on Power Systems* (Greece) and *Telkomnika Indonesian Journal of Electrical Engineering* (Indonesia). He serves as a reviewer of *Journal IEEE Transactions on SYSTEMS, MAN, AND CYBERNETICS*, *IEEE Transactions on Power Systems* (USA), *ETEP - European Transactions on Electrical Power Engineering* and *Journal of Zhejiang University SCIENCE (JZUS)*, China. He is associated with the Department of Electrical Engineering in Setif 1 University, Algeria. He currently serves as the President of the Scientific Council of the Department of Electrical Engineering and also a member of the Board of the University of Setif-1. He is also the responsible of the research team SMART GRID.